Celal Bayar University Journal of Science

An Investigation on the Flexural and Thermo-mechanical Properties of $CaCO_3$/Epoxy Composites

S. Bahar Baştürk[1]*

[1] Faculty of Engineering, Metallurgy and Materials Engineering Department, Manisa Celal Bayar University
*bahar.basturk@cbu.edu.tr
*Orcid: 0000-0002-4027-1935

Received: 27 October 2021
Accepted: 9 May 2022
DOI: 10.18466/cbayarfbe1015351

Abstract

Present work focused on the flexural and thermo-mechanical characteristics of epoxy based composites filled with 3 different calcium carbonate ($CaCO_3$) concentrations: 1.5, 3 and 5 wt.%. Composite specimens were fabricated through conventional casting method and subjected to flexural test via 3 point bending fixture. Additionally, dynamic-mechanical analyzer (DMA) with single cantilever mode was used to reval the thermo-mechanical responses of samples. The findings showed that the filler concentration increase led to the increase of storage modulus (E') for all specimens while the glass transition temperature (T_g) slightly decreased for 1.5 wt. % $CaCO_3$ filled epoxy composite. The 5 wt.% $CaCO_3$ loaded composite showed maximum E' and T_g values with 10% and 1.5% improvement, respectively. Based on flexural test results it was surprisingly found that, 1.5% wt. $CaCO_3$ addition attained the highest strength with ~30% improvement among all samples. However, 5 wt.% $CaCO_3$ introduced composites displayed the lowest mechanical performance due to the presence of agglomerates/tactoids, which was verified from SEM images as well.

Keywords: $CaCO_3$/epoxy composites, flexural properties, themo-mechanical response

1. Introduction

Application of polymer matrix composite (PMC) materials are extending day by day depending on the demands required by several markets like energy, automotive, aviation, electronics and infrastructure [1]. Epoxy is the mostly preferred thermoset matrix in composites due to its remarkable properties such as improved dimensional stability, high abrasion resistance and superior chemical resistance. Epoxies generally include two components (resin and hardener), and they attain desired stiffness via curing process, which is the transition from liquid to solid form in diverse durations [2-4]. When fibers or fillers integrated with epoxy, the resultant composites show exceptional mechanical strength and stiffness properties. In literature, various powders with micron or nano size (e.g., wood fiber, rice hull, sawdust, graphene oxide, magnesium hydroxide) have been introduced as the reinforcement phase to produce polymer matrix composites. Fundamentally, those powders are categorized into three main groups: natural, synthetic, and organic [5-6]. A large number of fillers such as talc, silica, clay, mica and $CaCO_3$ are industrially available and utilized in many areas. Among them, $CaCO_3$ is predominantly used because of its commercial abundance and low cost [7-9]. Mechanical, thermal and optical characteristics of polymers have been significantly enhanced with the addition of optimum $CaCO_3$ concentration. For instance, Techawinyutham et al. [5] investigated the performance of PP/$CaCO_3$ composites for 10, 20, 30 40 and 50 wt.% filler contents with and without maleic anhydride polypropylene (MAPP) introduction. They found that the strength values of composites decreased while tensile and flexural rigidities of the specimens increased. Azman et al. [10] examined the flexural responses of eggshell powder-ESP (as $CaCO_3$ source) filled epoxy composites loaded with 5, 10, 15 and 20 wt.% filler. Based on that study, 15 wt.% ESP concentration improved the modulus but led to lower strength as compared with neat epoxy. Kirboga et al. [11] developed biodegradable PHBV/$CaCO_3$ composites with 0.1-1 wt.% of $CaCO_3$ content and manufactured them by melt extrusion. According to their results, composite samples with 0.1wt.% $CaCO_3$ enhanced both storage and loss modulus values up to 76% and 175%, respectively. De Moura et al. [12] prepared composites by integrating 25 wt.% and

50 wt.% $CaCO_3$ and PU, separately. In that study, as the particle content increased, the tensile and flexural modulus of specimens increased while the strength values of composites improved only along out of plane direction.

Based on various studies referred above, it has been observed that nonidentical results were obtained with respect to filler concentration, particle form and size as well as experimental conditions. The main motivation of the present work is to reveal the effects of $CaCO_3$ filler on the flexural and thermo-mechanical characteristics of polymer composites. Indeed, the extended version of this study considers the utilization of low-cost micron size $CaCO_3$ powder with and without surface modification. However, as the first part, the content of the paper particularly covers the properties of composites including less amount unmodified $CaCO_3$ compared with literature [5,8,12]. Basically, $CaCO_3$ particles with 1.5, 3 and 5 wt.% concentration was dispersed in epoxy, casted into silicon molds and subjected to curing process. The produced composites were exposed to flexural test and dynamic mechanical analysis. Additionally, fractographic images of samples were evaluated to deeply understand the distribution of particles in the microstructure, which significantly affects the mechanical performance.

2. Materials and Methods

2.1. Materials

The thermoset epoxy matrix system consists of DTE 1200 resin and DTS 2110 hardener was purchased from Duratek™, Turkey. The calcium carbonate ($CaCO_3$) powder was provided by Merck™ with an average particle size of ~14 μm (d_{50}).

2.2. Preparation of Composites

In the present study, epoxy resin and micron sized $CaCO_3$ powder with 1.5, 3 and 5 wt.% were integrated with traditional casting method for composite production (see Figure 1). The required amount of DTE 1200 epoxy resin and $CaCO_3$ were blended firstly and dispersed in acetone for 3 hours. The mixture was dried at 80°C in the oven for 12 hours for acetone evaporation. Prior to casting, the DTS 2110 hardener was incorporated with mixture based on the manufacturer instructions and blended via magnetic stirrer for 30 minutes. Silicon moulds were filled with resultant composite mixture and kept into vacuum for minimizing void/bubble formation. Curing of samples were conducted at room temperature for 15 hours following a post-curing at 80 °C for 8 h. For simplicity, sample abbreviation adopted depending on filler volume fraction, e.g. 1.5$CaCO_3$-epoxy comp represents 1.5 wt.% $CaCO_3$ in epoxy matrix.

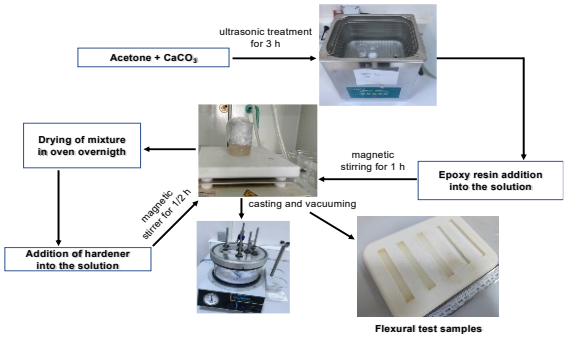

Figure 1: Preparation steps of flexural test samples.

2.3. Characterization of Composites

The X-ray diffraction (XRD) measurement of $CaCO_3$ powder was conducted via Panalytical Empyrean system with CuKα radiation (λ= 1.540Å) in a wide range of 2θ (10° ≤2θ ≤ 80°). The scanning speed of the diffractometer was fixed as 1°/min to disclose the crystalline properties and present phases. Flexural test of composites was performed in a universal mechanical test machine via three-point bending (3PB) fixture in accordance with ASTM D-790 standard [13] with a crosshead speed of 1.5 mm/min. Based on the standard, the full length was determined as 80 mm while the width (b) value of bending samples was determined as 14 mm. The thicknesses (d) of neat epoxy and the composite systems with 1.5%, %3 and %5 $CaCO_3$ content were measured as 4.23±0.08, 4.26±0.12, 4.21±0.10 and 4.23±0.14, respectively.

Flexural strength ($\sigma_{flexural}$) and modulus ($E_{flexural}$) parameters were calculated based on the equations (2.1) and (2.2) given below where span length (L) was specified as 64 mm.

$$\sigma_{flexural} = \frac{3PL}{2bd^2} \qquad (\mathbf{2.1})$$

$$E_{flexural} = \frac{L^3 m}{4bd^3} \qquad (\mathbf{2.2})$$

The "m" is the slope of the tangent to the initial straight-line portion of the load-deflection curve and obtained from the 3PB tests.

In this study, the visco-elastic responses of structures were characterized by dynamic-mechanical analyser (DMA) under liquid nitrogen atmosphere via TA™ Instrument Q800. Through DMA measurements, the variation of storage modulus (E') and loss modulus (E'') of every sample were recorded from 40°C to 150°C at 1 Hz constant frequency. Single cantilever mode was chosen and the heating rate was determined as 5°C/min. The E' and E'' represent the stored and dispersed energy values of specimens, respectively. The ratio of those two parameters (E''/E') is calculated by the analyzer and provide the "tangent delta-$tan\delta$" magnitude for each

Celal Bayar University Journal of Science
Volume 18, Issue 2, 2022, p 161-167
Doi: 10.18466/cbayarfbe1015351

temperature. Fracture surfaces of flexural test samples were investigated by scanning electron microscope (SEM) photographs taken by COXEM™ EM-30 Plus and Carl Zeiss 300 VP equipment.

3. Results and Discussion

3.1. XRD Results

Figure 2 shows the XRD patterns of as-received $CaCO_3$ powder in the 2θ range from 10° to 80°.The recorded diffraction peak locations, corresponding reflections, and calculated crystal size (or thickness) values of $CaCO_3$ powder are reported in Table 1. Debye–Scherrer equation is widely used to estimate the particle size of substances and expressed as in Eq. (3.1).

$$d = \frac{k\lambda}{\beta Cos\theta} \qquad (3.1)$$

Table 1. Debye–Scherrer parameters for the calculation of $CaCO_3$ crystal size.

2θ(°)	Reflection Planes	FWHM (radian)	Crystal size-d (μm)
29.25	(104)	0.001469	5.84
35.82	(110)	0.001494	5.85
39.26	(113)	0.001452	6.07
43	(202)	0.001373	6.50
47.35	(018)	0.001586	5.71
48.34	(116)	0.001513	6.02

The d, k, λ, β and $Cos\theta$ represent the crystal size, Debye–Scherrer constant (0.9), X-ray wavelength (0.15406 nm) and line broadening (in radian) found from the full width at half maximum (FWHM) of sharp peaks and Bragg angle, respectively [14]. According to the calculations, $CaCO_3$ crystal size values ranged between 5.7 μm to 6.5 μm, which is yet to be verified from SEM photos. By considering the findings from XRD analysis and based on the literature [15-16], it is concluded that calcite is the dominant phase for this powder (see Figure 2).

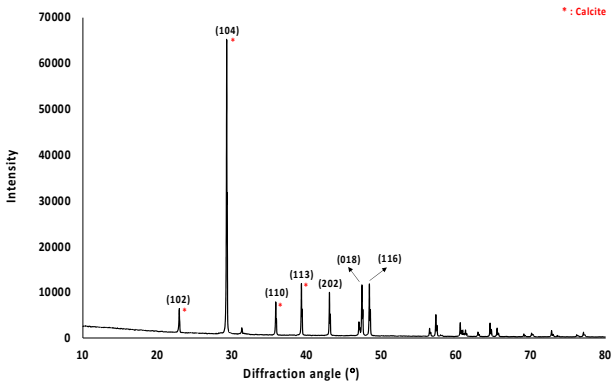

Figure 2. XRD patterns of $CaCO_3$.

3.2. Thermo-mechanical Results

The thermomechanical responses of $CaCO_3$/epoxy composites were determined via dynamic mechanical analyser (DMA) and the resultant graphs are shown in Figure 3 (a) to (c).

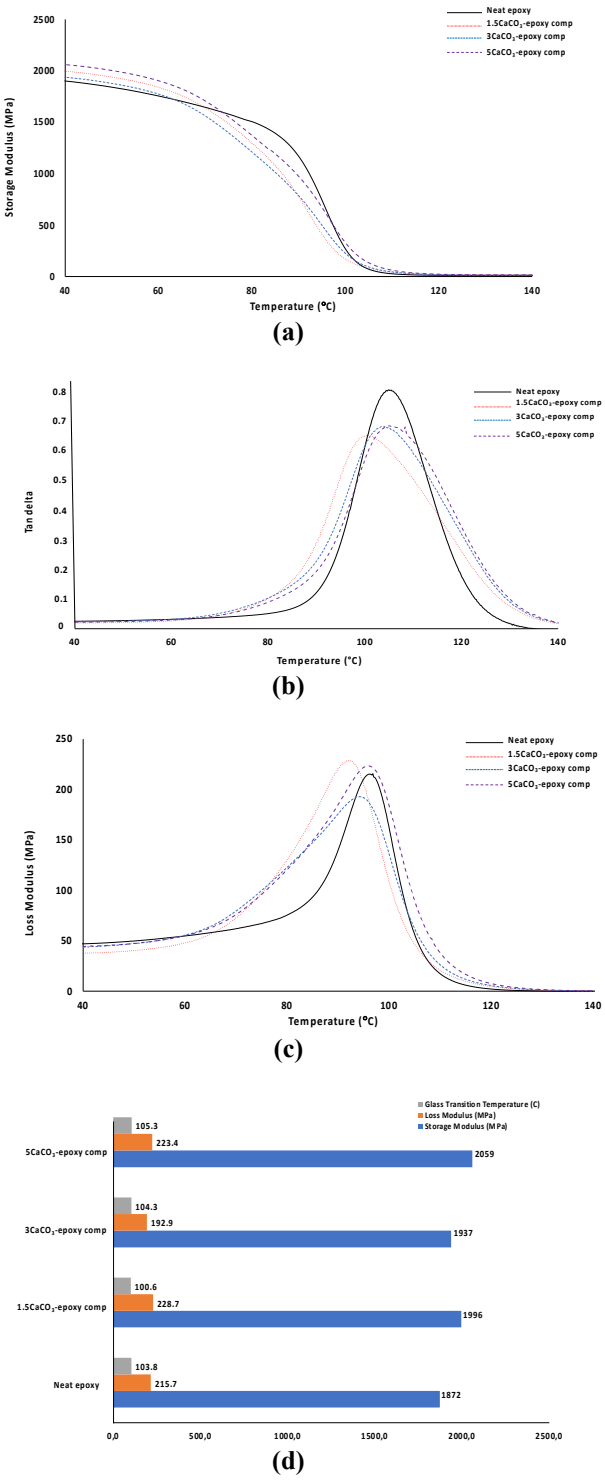

Figure 3. DMA results of $CaCO_3$/epoxy composites: a) E'-temperature variation, b) $tan\delta$-temperature variation, c) E''-temperature variation, d) Tg, E' and E'' variation depending on $CaCO_3$ concentration at 40°C.

Based on the theory of DMA, storage modulus (E') represents the elasticity of the material while loss modulus (E'') indicates the viscous characteristics of samples. The ratio between E' and E'' is expressed as the damping factor ($tan\delta$) and the peak point in $tan\delta$-temperature curve represents the glass transition temperature (T_g) of specimens [17]. Due to the temperature limitation and fluctuations during DMA analysis, the initial and final temperatures values were specified as 40°C and 140°C, respectively. The variations of glass transition temperature, storage modulus and loss modulus depending on $CaCO_3$ concentration are given as a different graph in Figure 3 (d). Storage modulus-temperature path generally follows three sequential sections: low temperature glassy zone, constricted steep decline zone and high temperature rubbery plateau [18]. All of those regions are available in Figure 3 (a) and as it is seen in the same figure that, at 40°C, the E' of pure epoxy exhibited the lowest value among all samples while the 5 wt. % filler loaded composite showed the highest storage modulus with 10% increase. Other two composites displayed close values for the same parameter at the same temperature. Therefore, increase of E' indicates the improved adhesion between filler and matrix. The rubbery plateau of the host matrix is appearently observed in Figure 3 (a), however, the addition of $CaCO_3$ led to the shrinkage of that plateau, as expected [17-18]. The increase in temperature caused to the enhancement of polymer chain mobility and resulted in the decrease of storage modulus, as in this study [18]. Based on Figure 3 (b), $tan\delta$ parameter reduced with the introduction of $CaCO_3$ powder independent of its amount, which indicates an advanced interaction between composite components [19]. Additionally, composite samples exhibit broader $tan\delta$ peaks that can be attributed to slower relaxation process due to matrix-filler interaction, as compared with pure epoxy [20].

The temperature corresponding to peak point of $tan\delta$ gives T_g, whose variation provides essential information about the effectiveness of particle-polymer bonding. For instance in this work, the $5CaCO_3$-epoxy composite exhibited maximum T_g (~1.5%↑) that is slightly higher than unfilled epoxy. However, 1.5 wt. % filler addition decreased that parameter into some extent and this situation may be related with the amount of micron-sizded filler that was insufficient for better interaction. It is also probable that nano-size $CaCO_3$ introduction with optimum content would result in higher glass transition temperature and/or storage modulus due to higher specific surface area of nano-particles [20]. Limited surface area of micron size filler considered in this study is presumably one of the main reasons for obtaining less effective results. In literature, Miranda et al. investigated [21] the thermo-mechanical characteristics of nano-$CaCO_3$/epoxy composites for 1, 2.5 and 5 wt.% particle content. Based on that study, the 2.5 wt. % filler concentration provided the maximum increase in T_g (from 137°C to 142°C with 5°C↑) with respect to neat epoxy. Nonetheless, the E' values of those samples were lower than epoxy matrix up to 120°C. Baskaran et al. [22] examined unsaturated polyester/nano-$CaCO_3$ composites for 1, 3, 5, 7 and 9 wt. % powder content. According to their study, 5 wt. % nanoparticle introduced composite achieved both maximum glass transition tempeature (from 90°C to 121°C with 31°C↑) and storage modulus among other composites.

Loss modulus (E'') describes the heat energy loss because of the internal friction occurs in polymers and composites during sinusoidal dynamic loading [23]. As the temperature enhanced, whole samples reached a maximum value for E'' and then dramatically dropped to zero when the polymer chain mobility becomes extremely high (transition from glassy state to rubbery state). The increase of loss modulus points out an advanced interfacial bonding between matrix and filler due to the enhanced energy dissipation between them [3,23]. In this work, only $3CaCO_3$-epoxy composite exhibited slightly lower E'' value, although its E' and T_g parameters were higher than host matrix.

3.3. Flexural Test Results

The effects of $CaCO_3$ content on the flexural properties of composites are presented in Figure 4 (a) and (b) with representative samples.

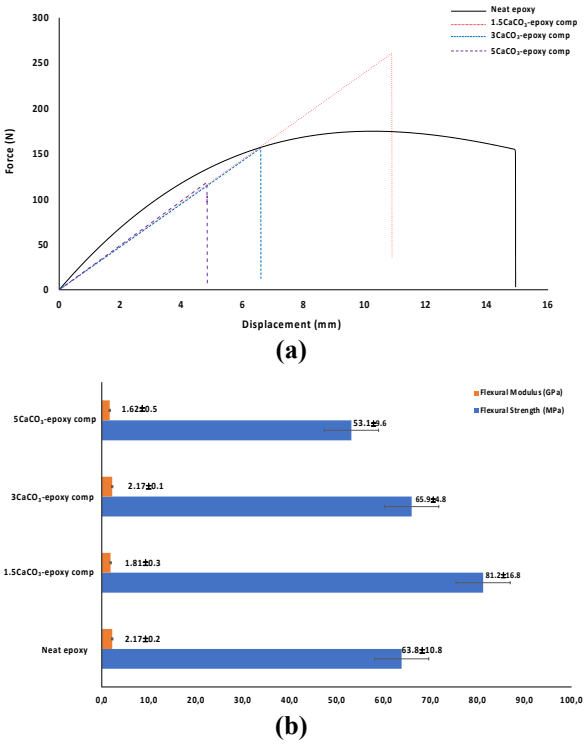

Figure 4. (a) Flexural force-displacement graph, (b) average flexural modulus and strength variation of $CaCO_3$/epoxy composites depending on $CaCO_3$ concentration.

As obviously seen in that figure, addition of $CaCO_3$ resulted in the increase of brittle character and caused to the decrease of plasticity in composites (see Figure 4-a). The calculated mechanical parameters such as flexural strength and modulus are given in Figure 4 (b) with standard deviations. Based on that figure it is interestingly observed that, the 1.5% wt. $CaCO_3$ introduction achieved the maximum strength (81.2 MPa with ~30% improvement) but reduced the flexural modulus (1.81 GPa with 17% decline) as compared with neat epoxy. Additionally, the 3% wt. $CaCO_3$ showed slightly higher strength (65,9 MPa with 3% improvement) and modulus (2.18 GPa with 1% improvement) values than matrix material. However, 5 wt.% $CaCO_3$ loaded composites exhibited lowest mechanical properties due to the presence of agglomerates, which is yet to be confirmed from SEM images. It is probable that 5% wt. filler in the matrix was excessive in terms of optimum flexural properties while the other two concentrations facilitated better reinforcement-matrix interaction.

Suresha et al. [2] prepared the nano-$CaCO_3$/epoxy composites for 1,3 and 5 wt.% particle content and according to that study, both stiffness and strength magnitudes of samples decreased under out of plane loading. Likewise, Yang et al. [24] investigated the cube-like $CaCO_3$ introduced epoxy composites and they found that 1.5 wt.% filler presence led to the maximum improvement in flexural properties. Eskizeybek et al. [25] integrated epoxy with 1, 2 and 3 wt.% nano-$CaCO_3$ powder and based on that research, 2 wt.% filler exhibited the maximum performance both in tensile and flexural loading.

3.4. Fractographic Analysis

The SEM images of $CaCO_3$, neat epoxy and composites after flexural test are shown in Figure 5. The cubic morphology of $CaCO_3$ particles is apparently seen in Figure 5 (a) and it is also clear that those cubes in the photos show large size variations. The micron-size filler clusters form agglomerates and are present in the other figures as well. It is obvious that the 1.5 wt.% $CaCO_3$ loaded composite displayed rougher fracture surface than other composites (see Figures 5-c, 5-e and 5-g) that can be attributed to more energy absorption and relatively fine particle dispersion. Approximately 30% flexural strength improvement can be related with this situation occurred in the microstructure.

Additionally, pit formation is seen in the inset of Figure 5 (e) and this defect can be attributed to the detachment of filler from matrix material. As observed from the insets of Figure 5 (d), (f) and (h) that, the agglomerates thoroughly embedded in the microstructure, which points out an advanced bonding between epoxy and $CaCO_3$. Despite this positive effect, filler concentration increase caused to the existence/increase of cluster formation. In particular, non-homogeneous powder distribution was observed with the introduction of 3 wt.% and 5 wt.% $CaCO_3$, which resulted in the reduction of stress transfer between matrix and reinforcement phase [17].

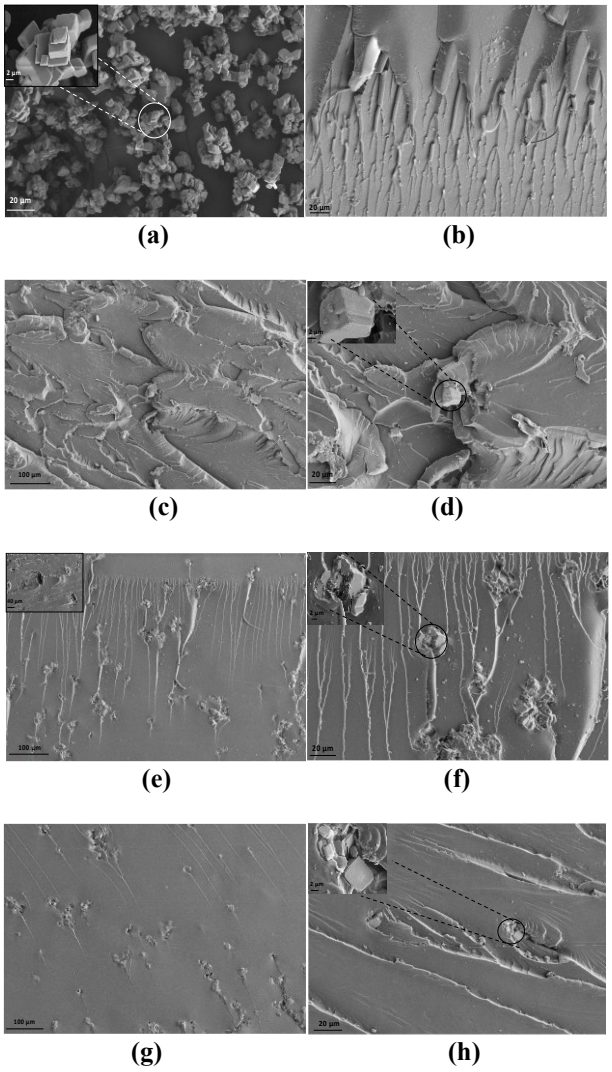

Figure 5. SEM images of a) neat $CaCO_3$, b) neat epoxy, c)1.5$CaCO_3$-epoxy composite (100 µm scale), d)1.5$CaCO_3$-epoxy composite (20 µm scale), e) 3$CaCO_3$-epoxy composite (100 µm scale), f) 3$CaCO_3$-epoxy composite (20 µm scale), g) 5$CaCO_3$-epoxy composite (100 µm scale), h) 5$CaCO_3$-epoxy composite (20 µm scale).

4. Conclusions

In the context of the present study, cube shaped $CaCO_3$ particles with 1.5, 3 and 5 wt.% content was dispersed in epoxy medium. The samples fabricated with traditional casting technique were considered in terms of their thermo-mechanical and flexural responses via dynamic-mechanical analyzer (DMA) and three-point bending fixture, respectively. According to XRD

analysis, calcite was detected as the dominant phase in cubic $CaCO_3$ particles and the crystal size of powder was approximated between 5.7 µm to 6.5 µm, which was also confirmed by SEM measurements. Based on DMA results, the 5 wt.% filler content provided the maximum values in terms of storage modulus (E') and glass transition (T_g) temperature. It was interestingly found that the 3 wt.% $CaCO_3$ presence resulted in the lowest loss modulus (E'') despite its improved E' and T_g values as compared with epoxy matrix. Flexural test results revealed that 1.5 wt. % $CaCO_3$ addition enhanced the strength parameter of about 30% while the modulus slightly decreased for the same concentration. The observations from SEM fracture images, it was concluded that, filler amount increase (for 3 wt. % and 5 wt. %) caused to the $CaCO_3$ agglomeration, which was evaluated as an indication for the reduced strength. To overcome that negative situation, it is planned to apply silane and/or oleic acid modification to filler in the second part of the study. With the introduction of a surface agent, hydrophilicity of calcite will probably decrease, which leads to better dispersity in the matrix.

Author's Contributions

S. Bahar Baştürk: Drafted and wrote the manuscript, performed, and interpreted the whole experiments and analysis.

Ethics

There are no ethical issues after the publication of this manuscript.

References

[1]. Türkmen, İ, Köksal, N.S. 2013, Investigation of mechanical properties and impact strength depending on the number of fiber layers in glass fiber reinforced polyester matrix composite materials. *CBU Journal of Science*; 8(2): 17-30.

[2]. Suresha, B, Varun, C.A, Indushekhara, N.M, Vishwanath, H.R, Venkatesh. 2019. Effect of Nano filler reinforcement on mechanical properties of epoxy composites. *IOP Conf. Series: Materials Science and Engineering;* 574, 012010.

[3]. Ho, NM, Nguyen, TC, Tran, TTV, Nguyen, TD, Thai, H. 2021. Enhancement of dynamic mechanical properties and flame resistance of nanocomposites based on epoxy and nanosilica modified with KR-12 coupling agent. *Journal of Applied Polymer Science;* 138(29): 50685.

[4]. Xian, Y, Kang, Z, Liang, X. 2021. Effect of nanodiamonds and multi-walled carbon nanotubes in thermoset hybrid fillers system: Rheology, dynamic mechanical analysis, and thermal stability. *Journal of Applied Polymer Science*; 138(21): 50496.

[5]. Techawinyutham, L, Sumrith, N, Srisuk, R, Techawinyutham, W, Siengchin, S, Mavinkere Rangappa, S. 2021. Thermo-mechanical, rheological and morphology properties of polypropylene composites: Residual $CaCO_3$ as a sustainable by-product. *Polymer Composites*; 42(9): 4643.

[6]. Poyraz, B, Eren, Ş, Subaşı, S. 2020. Filler type and particle distribution effect on compact properties of polymer composites. *CBU Journal of Science*; 17(1): 79-89.

[7]. Kapusuz, D, Ercan, B. 2019. Calcium phosphate mineralization on calcium carbonate particle incorporated silk-fibroin composites. *CBU Journal of Science*; 15(3): 301-306.

[8]. Tao, Y, Mao, Z, Yang, Z, Zhang, J. 2021. $CaCO_3$ as a new member of high solar-reflective filler on the cooling property in polymer composites, *Journal of Vinyl and Additive Technology*; 27(2): 275– 287.

[9]. Yao, J, Hu, H, Sun, Z, Wang, Y, Huang, H, Gao, L, Jiang, X, Wang, X, Xiong, C. 2021. Synchronously strengthen and toughen polypropylene using tartaric acid-modified nano-$CaCO_3$. *Nanomaterials*; 11(10):2493.

[10]. Azman, N.A.N, Islam, M.R, Parimalam, M. 2020. Mechanical, structural, thermal and morphological properties of epoxy composites filled with chicken eggshell and inorganic CaCO3 particles. *Polymer Bulletin*; 77: 805–821.

[11]. Kirboga, S, Öner, M, Deveci, S. 2021. Preparation and characterization of calcium carbonate reinforced poly(3-hydroxybutyrate-co-3-hydroxyvalerate) biocomposites. *Current Nanoscience*; 17(2): 266-278.

[12]. De Moura A.P, Da Silva E.H, Dos Santos V.S. 2021. Structural and mechanical characterization of polyurethane-CaCO3 composites synthesized at high calcium carbonate loading: An experimental and theoretical study. *Journal of Composite Materials*; doi:10.1177/0021998321996414.

[13]. American Society for Testing and Materials, ASTM D790, 2004. Standard Test Methods for Flexural Properties of Unreinforced and Reinforced Plastics and Electrical Insulating Materials.

[14]. Bokuniaeva, A.O, Vorokh, A.S. 2019. Estimation of particle size using the Debye equation and the Scherrer formula for polyphasic TiO_2 powder. *Journal of Physics: Conference Series;* 1410, 012057.

[15]. Mallakpour, S, Khadem, E. 2017. Facile and cost-effective preparation of PVA/modified calcium carbonate nanocomposites via ultrasonic irradiation: Application in adsorption of heavy metal and oxygen permeation property. *Ultrasonics Sonochemistry*; 39: 430–438.

[16]. Tran, H.V, Tran, L.D, Vu, H.D, Thai, H. 2010. Facile surface modification of nanoprecipitated calcium carbonate by adsorption of sodium stearate in aqueous solution. *Colloids and Surfaces A: Physicochemical and Engineering Aspects*; 366(1–3): 95–103.

[17]. Menard, K.P. Dynamic Mechanical Analysis: A Practical Introduction, Second Edition (2nd ed.), CRC Press, 2008; pp 91.

[18]. Panwar, V, Pal, K. Dynamic Mechanical Analysis of Clay-Polymer Nanocomposites. In Clay-Polymer Nanocomposites, 1st edn. Elsevier, New York, 2017, pp 413–441.

[19]. Bashir, M.A. 2021. Use of Dynamic Mechanical Analysis (DMA) for Characterizing Interfacial Interactions in Filled Polymers. *Solids*; 2, 108-120.

[20]. Fombuena, V, Bernardi, L, Fenollar, O, Boronat, T, Balart, R. 2014. Characterization of green composites from biobased epoxy matrices and bio-fillers derived from seashell wastes. *Materials and Design*; 57, 168–174.

[21]. Miranda, T.B, Silva G.G. 2020. Hierarchical microstructure of nanoparticles of calcium carbonate/epoxy composites: thermomechanical and surface properties. *Express Polymer Letters*; 14:179–191.

[22]. Baskaran, R, Sarojadevi, M, Vijayakumar, C.T. 2011. Mechanical and thermal properties of unsaturated polyester/calcium carbonate nanocomposites. *Journal of Reinforced Plastics and Composites*; 30(18):1549-1556.

[23]. Mat Yazik, M.H, Sultan, M.T.H, Jawaid, M, Abu Talib, A.R, Mazlan, N, Md Shah, A.U, Safri, S.N.A. 2021. Effect of nanofiller content on dynamic mechanical and thermal properties of multi-walled carbon nanotube and montmorillonite nanoclay filler hybrid shape memory epoxy composites. *Polymer*s; 13, 700.

[24]. Yang, G, Heo, Y.-J, Park, S.-J. 2019. Effect of morphology of calcium carbonate on toughness behavior and thermal stability of epoxy-based composites. *Processes;* 7, 178.

[25]. Eskizeybek, V, Ulus, H, Kaybal, H. B, Şahin, Ö. S, Avcı, A. 2018. Static and dynamic mechanical responses of $CaCO_3$ nanoparticle modified epoxy/carbon fiber nanocomposites. *Composites Part B: Engineering*; 140, 223–231.